

Differences in the ionic interaction of actin with the motor domains of nonmuscle and muscle myosin II

Juliette Van Dijk¹, Marcus Furch², Jean Derancourt¹, Renu Batra², Menno L. W. Knetsch², Dietmar J. Manstein² and Patrick Chaussepied¹

¹UPR 1086 du CNRS, Montpellier, France; ²Max-Planck-Institut für Medizinische Forschung, Heidelberg, Germany

Changes in the actin–myosin interface are thought to play an important role in microfilament-linked cellular movements. In this study, we compared the actin binding properties of the motor domain of *Dictyostelium discoideum* (M765) and rabbit skeletal muscle myosin subfragment-1 (S1). The *Dictyostelium* motor domain resembles S1(A2) (S1 carrying the A2 light chain) in its interaction with G-actin. Similar to S1(A2), none of the *Dictyostelium* motor domain constructs induced G-actin polymerization. The affinity of monomeric actin (G-actin) was 20-fold lower for M765 than for S1(A2) but increasing the number of positive charges in the loop 2 region of the *D. discoideum* motor domain (residues 613–623) resulted in equivalent affinities of G-actin for M765 and for S1. Proteolytic cleavage and cross-linking approaches were used to show that M765, like S1, interacts via the loop 2 region with filamentous actin (F-actin). For both types of myosin, F-actin prevents trypsin cleavage in the loop 2 region and F-actin segment 1–28 can be cross-linked to loop 2 residues by a carbodiimide-induced reaction. In contrast with the S1, loop residues 559–565 of *D. discoideum* myosin was not cross-linked to F-actin, probably due to the lower number of positive charges. These results confirm the importance of the loop 2 region of myosin for the interaction with both G-actin and F-actin, regardless of the source of myosin. The differences observed in the way in which M765 and S1 interact with actin may be linked to more general differences in the structure of the actomyosin interface of muscle and nonmuscle myosins.

Keywords: actin; myosin; actomyosin interface; cross-linking; proteolysis; adenosinetriphosphatase; mutagenesis.

The mechanical energy produced by myosin II drives muscle contraction and many fundamental processes such as the capping of cell surface receptors, cytokinesis, and a variety of other motile events. The molecular basis of this force resides in the cyclical interaction between filamentous actin and myosin. In fact, the catalytic activity of myosin is located in the highly conserved motor domain which interacts with actin, binds to and hydrolyses ATP and produces the force for movement along actin filaments. The three-dimensional structures of the motor domains of different members of myosin class II share remarkable identity [1]. The data on the kinetics of ATP hydrolysis obtained from at least three classes of myosin could be fitted using a similar kinetic scheme. This suggests a unity in the molecular mechanism of the mechanochemical transduction process by myosin molecules [2–5]. However, differences in catalytic efficiency between the various myosins do exist and are not well understood at the molecular level. The rate of movement induced by myosins of class II can vary by a factor of 100 or more when compared under the same ionic conditions [6].

Correspondence to P. Chaussepied, UPR 1086 du CNRS, 34293 Montpellier, Cedex5, France. Tel: + 33 4 67 61 33 34. Fax: + 33 4 67 52 15 59.

E-mail: Patrick@crbm.cnrs-mop.fr

Abbreviations: EDC, 1-ethyl-3[3-(dimethylamino)-propyl]-carbodiimide; 1,5-IAEDANS, N-(iodoacetyl)-N'-(5-sulfo-1-naphthyl)ethylenediamine; M765, residues 1–765 of *Dictyostelium discoideum* myosin motor domain; NHS, N-hydroxysuccinimide; S1(A1), S1(A2), skeletal muscle myosin subfragment-1 with alkali light chain A1 or A2, respectively.

Enzymes: Myosin ATPase (EC 3.6.1.32); Chymotrypsin (EC 3.4.21.1); Trypsin (EC 3.4.21.4).

(Received 17 September 1998, revised 8 December 1998, accepted 8 December 1998)

The three-dimensional reconstruction of the actin–myosin motor domain complex suggests very similar interfaces for skeletal muscle and *Dictyostelium discoideum* myosin II [7–9]. Careful analysis of the primary sequences of four actomyosin contact sites revealed notable differences in the number of charged residues and in the length of two sequence segments in the actin-binding region of myosin [8].

The first actin-binding segment corresponds to loop 2 (residues 613–623 of *D. discoideum* myosin sequence). Work performed on muscle myosin head fragments gave convincing experimental evidence for loop 2 acting as one of the major components of the so-called weak interface (in the presence of ATP or the hydrolysed ADP.Pi intermediate). However, the contribution of loop 2 to the strong (or rigor) interface (with ADP or without nucleotide) was questioned in several studies [10–13]. Genetic replacements within the loop 2 segment affected actin-activated ATPase activity as well as the regulation of the myosin ATPase activity [14,15]. Recently, the modulation of actin affinity and actomyosin ATPase activity by charge and length changes in the loop 2 regions was dissected in a study involving nine mutant constructs of the *D. discoideum* myosin II motor domain [16]. A further surface segment of the myosin head (residues 565–575 of *D. discoideum*) was first proposed to participate in a secondary binding event with an adjacent monomer [8]. Using chemical cross-linking approaches, this region was recently implicated in the formation of a weak binding interaction between F-actin and skeletal muscle myosin [17].

To characterize the interaction between actin and myosin further, we compared the actin-binding properties of M765, the recombinant motor domain of *D. discoideum* myosin II, and S1 from rabbit skeletal muscle. M765 has been shown to retain normal ATP-hydrolysis and actin-binding activities [18].

Additionally, construct M761-2R was used in this study. M761-2R, which has the regulatory domain replaced by two α -actinin repeats, moves actin at similar rates as the full length motor domain (M864) in an *in vitro* motility system [19]. Skeletal muscle myosin S1 was produced by the chymotryptic cleavage of muscle myosin at residue 840. Depending on the nature of the alkali light chain, two S1 isoforms, S1(A1) and S1(A2), can be obtained. These two isoenzymes are characterized by different ATPase activities at low ionic strength [20], different efficiencies in *in vitro* motility assays [21], and in muscle fibres [22]. They also display large differences in their capability to induce polymerization of monomeric actin [23,24].

Using spectroscopic measurements in combination with proteolytic and chemical cross-linking experiments, this study reveals that the ability of a myosin to bind to G-actin and to F-actin depends on the number of charges present in loop 2. It is also shown that besides the differences at the interface between actin subdomain 1 and myosin loop 2, nonmuscle and muscle myosin display significant differences in other ionic contacts with filamentous actin.

MATERIALS AND METHODS

Materials

Trypsin, 1-(3-dimethylaminopropyl)-3-ethylcarbodiimide (EDC), N-hydroxy-succinimide (NHS), N-(iodoacetyl)-N'-(5-sulfo-1-naphthyl)ethylenediamine (1,5-IAEDANS), ADP, thrombin from human plasma (200 U·mg⁻¹), antipolyhistidine and anti-rabbit and antimouse IgG antibodies labelled with peroxidase were purchased from Sigma. α -Chymotrypsin, V-8 protease and sodium vanadate were from Worthington Biochemicals, ICN Biomedicals and Aldrich, respectively. NaF, BeSO₄ and AlCl₃ were from Merck. ATP, soybean trypsin inhibitor, endoproteinase Arg-C, and subtilisin were obtained from Boehringer Mannheim. PD-10 columns and Sephacryl 200 were supplied by Pharmacia. All other chemicals were of analytical grade.

Preparation of proteins

Rabbit skeletal myosin was prepared as described by Offer *et al.* [25]. S1 was obtained by chymotryptic digestion of myosin filaments [26]. Both isoforms S1(A1) and S1(A2) were separated by ion exchange chromatography as described previously [24].

Rabbit skeletal F-actin was prepared from acetone powder and further purified by two cycles of polymerization/depolymerization [27]. G-actin was equilibrated in buffer G₅₀ (5 mM Hepes, 0.1 mM CaCl₂, 50 μ M ATP, pH 8.0). Subtilisin-actin was generated by proteolysis of G-actin with subtilisin for 15 min at an enzyme/substrate weight ratio of 1 : 2000. The digestion was stopped with 4 mM phenylmethanesulfonyl fluoride. Polymerization of cleaved and uncleaved actin was achieved by the addition of 0.1 M KCl, 2 mM MgCl₂ for 1–2 h at 25 °C. Protein concentrations were determined spectrophotometrically using extinction coefficients of A^{1%}_{280nm} = 5.7 cm⁻¹ for myosin, 7.5 cm⁻¹ for S1 and 11.0 cm⁻¹ for actin. The molecular masses used were 500 kDa, 115 kDa and 42 kDa for myosin, S1 and actin, respectively.

M765 and M761-2R derivatives were engineered, expressed in *D. discoideum* and purified as described by Manstein and Hunt [28] and Anson *et al.* [19], respectively. M761(0/-3)-2R was created by PCR-directed mutagenesis of M761-2R. The molecular masses used were 88 kDa for M765, M765(8/+4), and M765(11/+6) and 115 kDa for the constructs with the two

α -actinin repeats, M761-2R and M761(0/-3)-2R. Protein concentrations of M765 constructs were estimated according to Bradford [29].

Modification of actin by 1,5-IAEDANS

F-actin (in 50 mM Hepes, 100 mM KCl, 5 mM MgCl₂, pH 7.0) was incubated for 1 h at 20 °C with a 10-fold molar excess of 1,5-IAEDANS. The reaction was stopped by 50 mM 2-mercaptoethanol. After ultracentrifugation at 380000 g for 15 min, F-actin was depolymerized in G₅₀ buffer and purified on a PD-10 column equilibrated with buffer G₅₀ as described previously [24]. The extent of labelling was determined by using a molar extinction coefficient of E_{335nm} = 6200 M⁻¹·cm⁻¹.

Proteolytic digestions

Digestions of myosin motor domains by Arg-C, V8, trypsin and chymotrypsin were carried out at 25 °C with 20 μ M S1 in 10 mM Hepes (pH 8.0) with a protease to motor domain weight ratio of 1 : 50 in the presence or in the absence of 40 μ M F-actin. Alternatively, digestions were performed after a 15-min incubation with 2 mM ADP alone or in the presence of 10 mM NaF and 2 mM BeSO₄ to form ADP·BeF_x, 10 mM NaF and 2 mM AlCl₃ to form ADP·AlF₄⁻ and 2 mM VO₄³⁻ (stock solution prepared according to Goodno [30]) to form ADP·VO₄³⁻ complexes bound to the myosin motor domain. For digestions in the presence of ATP, 20 mM nucleotide was added to the mixture prior to the protease. The proteolysis reaction was stopped after 20 min by incubating an aliquot of each reaction mixture with 3 vols of boiling Laemmli's buffer [31]. The results of the proteolysis were visualized by gel electrophoresis.

M765 trypsin derivatives were produced at 25 °C in 10 mM Hepes (pH 8.0) by reaction of 50 μ M M765 or M765(8/+4) with trypsin at an enzyme to substrate weight ratio of 1 : 50. The proteolytic reaction was stopped by the addition of a twofold excess of soybean trypsin inhibitor over trypsin after 20 or 45 min for M765(8/+4) and M765, respectively.

Binding experiments

The interaction between motor domains and 1,5-IAEDANS–G-actin was studied at 20 °C in buffer G₅₀ (under nonpolymerizing conditions) using the increase in the polarization of the IAEDANS chromophore induced by the formation of G-actin–motor domain complex. Data were recorded after each consecutive addition of motor domain derivatives to a solution containing 2 μ M 1,5-IAEDANS–G-actin. The binding curves were computed using the software Graphpad PrismTM and calculation of the dissociation constants was performed assuming one binding site, using the equation:

$$Y = Y_0 + Y_m[u - (u^2 - x/p)^{-2}]$$

in which Y is the polarization for a chosen motor domain concentration (x), Y_0 and Y_m , the polarization of G-actin alone and totally saturated by motor domain, respectively, and:

$$u = (x + K_d + p)/2p$$

with K_d , the dissociation constant and p , the initial IAEDANS–G-actin concentration.

Cross-linking of M765 derivatives to actin derivatives

F-actin, IAEDANS–F-actin or subtilisin–F-actin in cross-linking buffer (30 mM Mops, 2.5 mM MgCl₂, pH 7.0 at 25 °C) was

mixed with M765 or its tryptic (68–16.5/15.5 kDa)-M765 derivative at an actin to M765 ratio of 3 : 1. The cross-linking reaction was initiated by addition of 15 mM NHS and EDC (freshly dissolved in the cross-linking buffer). For time course analysis, reactions were terminated at the times indicated by the addition of Laemmli's buffer and the content of the reaction mixture was analysed by SDS/PAGE. For proteolytic analysis of the cross-linked actin–M765 complexes, cross-linking reactions were stopped after 20 min by the addition of 50 mM 2-mercaptoethanol and 200 mM glycine.

Alternatively, cross-linking reactions were conducted using a two-step process to protect the integrity of M765 for measurements of the ATPase activities of cross-linked actin–M765 complexes. First, 60 μ M actin in cross-linking buffer was activated by 20 mM EDC in the presence of 50 mM NHS for 15 min at 25 °C. The activation was stopped by the addition of 50 mM 2-mercaptoethanol and the cross-linking reaction was initiated by the addition of 10 μ M M765 (final actin concentration 30 μ M). After 30 s or 60 s, an aliquot was withdrawn and either mixed with 2 vols boiling Laemmli's buffer for SDS/PAGE analysis or quenched by the addition of 200 mM glycine for Mg²⁺-ATPase measurements. The amount of noncross-linked M765 was estimated by gel scanning.

Cross-linking reactions between G-actin (8 μ M) and M765 (8 μ M) were performed in buffer G₅₀ at 10 °C to avoid uncontrolled polymerization of the G-actin–M765 complexes. Cross-linking reactions were initiated by adding 2.5 mM NHS and EDC and the samples were withdrawn from the cross-linking mixtures after 45 min for SDS/PAGE. In all experiments, NHS and EDC were freshly dissolved in the appropriate buffer.

Proteolytic cleavage of the cross-linked actin–M765 complexes

In order to digest the covalent actin–M765 complexes by thrombin, noncross-linked M765 was first eliminated from the reaction mixture by the addition of an equal volume of dissociating buffer (100 mM Tris, 1.5 M NaCl, 10 mM MgCl₂, 20 mM NaPP_i, 10 mM ATP, pH 8.0) followed by centrifugation for 15 min at 380 000 *g* and 4 °C. The covalent complexes present in the pellet were depolymerized for 30 min at 0 °C in 0.6 M KI, 20 mM Tris, 2 mM EDTA, 0.5 mM ATP, pH 8.0 and subjected to three sonifications of 1 min each at a frequency of 20 kHz in a Microson cell disruptor (model XL 2005;). The sample was passed through a PD-10 column against EDTA-containing buffer (4 mM Hepes, 1 mM EDTA, 0.5 mM ATP, pH 8.0) and concentrated in an Amicon Cell (PM30 membrane) and treated with thrombin at a complex to protease weight ratio

of 1 : 30 for 20 min at 25 °C. The digestion was stopped by the addition to 3 vols of boiling Laemmli's buffer, at the times indicated.

SDS/PAGE and Western blot analysis

Gel electrophoresis was performed as described by Laemmli [31] using 4–18% gradient acrylamide gels. Densitometric analysis of the Coomassie blue-stained gels was carried out with a Shimadzu CS 930 high-resolution gel scanner equipped with a computerized integrator. Western blot analysis using rabbit polyclonal antibodies directed against M765 or mouse monoclonal antipolyhistidine tag was performed as described [32].

Spectral measurements

Light scattering and fluorescence polarization measurements were carried out on a Kontron SFM 25 spectrofluorimeter or an SLM Aminco thermostated at 25 °C. Prior to the measurements, all samples and buffers were passed through a 0.45- μ m Millipore filter. Light scattering intensity was monitored at 90° to the incident light at a wavelength of 400 nm. Fluorescence polarization measurements were monitored at 467 nm with the excitation wavelength at 360 nm.

Sequence analysis

N-terminal sequence determination of the different proteolytic fragments was achieved after gel electrophoresis and electro-transfer of the fragments onto a poly-vinylidene difluoride membrane. The membrane was then subjected to N-terminal sequencing using a Perkin-Elmer Procise 492 sequencer operated according to the manufacturer's pulsed liquid program.

ATPase measurements

ATPase activity of G-actin–M765 complexes (8 μ M) was estimated at 25 °C as described [33,34] by following the change of intrinsic fluorescence during the reaction performed in buffer G (5 mM Hepes, 0.1 mM CaCl₂, pH 8.0). The solution was excited at 300 nm and tryptophan fluorescence was monitored at 336 nm. The reaction was initiated by the addition of 20 μ M ATP.

The F-actin-activated Mg²⁺-ATPase activity was measured at 25 °C in 50 mM Tris, 2.5 mM MgCl₂, 10 mM KCl, pH 8.0 in the presence of 2 mM ATP. The values obtained are the means of two to four independent determinations. The amount of P_i liberated was evaluated colorimetrically as described [35].

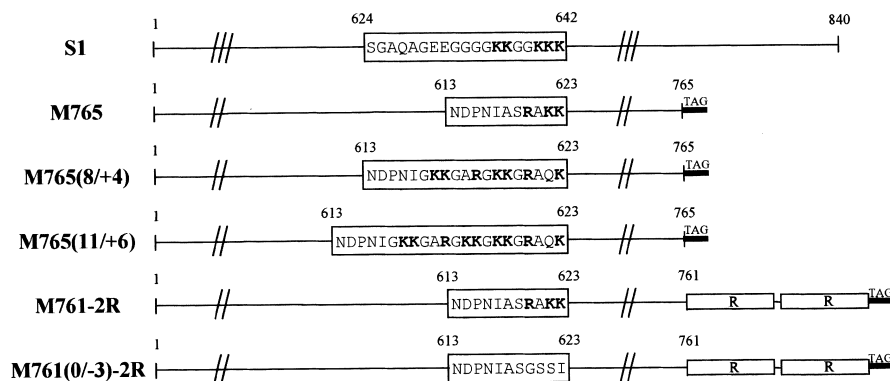


Fig. 1. Schematic representation of the different myosin motor domains. The myosin motor domain of rabbit skeletal muscle (S1) and *D. discoideum* (M765) as well as the four mutant M765 constructs are represented. All myosins from *D. discoideum* have a C-terminal tag [Ala-Leu-(His)₈]. The last two constructs are fused to two α -actinin repeats (R, residues 264–505 of *D. discoideum* α -actinin) via a linker (Leu-Gly-Ser). The amino acid sequences of loop 2 are indicated in the boxes. The naming of the mutant motor domain constructs are as in Furch *et al.* [16] with the changes in length and charge indicated in parenthesis.

RESULTS

The actin binding properties of S1 isoforms, S1(A1) and S1(A2) were compared with those of five *D. discoideum* myosin II motor domain constructs (Fig. 1). The *D. discoideum* mutant constructs M765(8/+4) and M765(11/+6) differ from wild-type M765 by the introduction of four and six additional positively-charged residues in loop 2 (residues 613–623), respectively. M761-2R corresponds to the first 761 residues of *D. discoideum* myosin II fused to two α -actinin repeats via a tripeptide linker (Leu-Gly-Ser) and M761(0/-3)-2R is a similar construct in which the positively-charged residues of loop 2 have been replaced by uncharged residues. The addition of two α -actinin repeats to the *D. discoideum* myosin II motor domain produces a molecular motor with actin motility properties that are similar to or greater than those of the native myosin [19]. All *D. discoideum* constructs contain a histidine tag at their C-termini to allow purification by Ni-chelate-chromatography [16].

Interaction of the myosin motor domain with monomeric actin

Muscle myosin and S1 derivatives are known to bind strongly to G-actin and to induce its polymerization in low salt buffer (buffer G₅₀). It was reported however, that S1(A1) can induce G-actin polymerization at a much lower protein concentration

than S1(A2) [23,24]. To compare the polymerization properties of M765 with those of S1 isoforms, we followed the changes in light scattering of G-actin upon addition of either M765 or S1 derivatives (Fig. 2A). Polymerization of 8 μ M G-actin in the presence of 8 μ M S1(A1) at 25 °C in buffer G₅₀ was characterized by a short stationary phase followed by a slow increase of the scattered light as described previously [24]. Complete polymerization of the sample, at maximum light scattering, was confirmed by the presence of only trace amounts of protein in the supernatant after ultracentrifugation of the solution (not shown). As expected at this protein concentration, addition of S1(A2) did not significantly change the value of light scattering of the solution and did not induce G-actin polymerization unless salt, such as MgCl₂, was added (Fig. 2A, dashed line). Like S1(A2), none of the M765 constructs induced actin polymerization in the absence of salt, regardless of the number of charges present in the loop 2 segment (Fig. 2A, dotted and solid lines). Differences in scattering intensity, observed upon addition of S1 derivatives, were probably due to differences in the intrinsic scattering of individual S1 samples. Addition of MgCl₂ always lead to a more rapid increase of light scattering in the presence of M765 derivatives than with S1(A2). This faster polymerization may reflect a more efficient stabilization of the nascent actin filament by M765.

The failure of the recombinant *D. discoideum* motor domains to induce actin polymerization is not due to their inability to bind to G-actin, as the addition of both M765 and M765(11/+6) to 1,5-IAEDANS-G-actin is followed by a rapid enhancement of the fluorescence polarization (Fig. 2B). This behaviour is similar to that observed with S1(A2). In these three cases, the polarization value of the actin-S1 complex was stable. Addition of MgCl₂ induced a further signal increase to a value characteristic for polymerized 1,5-IAEDANS-F-actin [36]. The initial increase of polarization was lower with M765 than with M765(11/+6). This difference was interpreted as a lower amount of G-actin-M765 complex formed under these conditions.

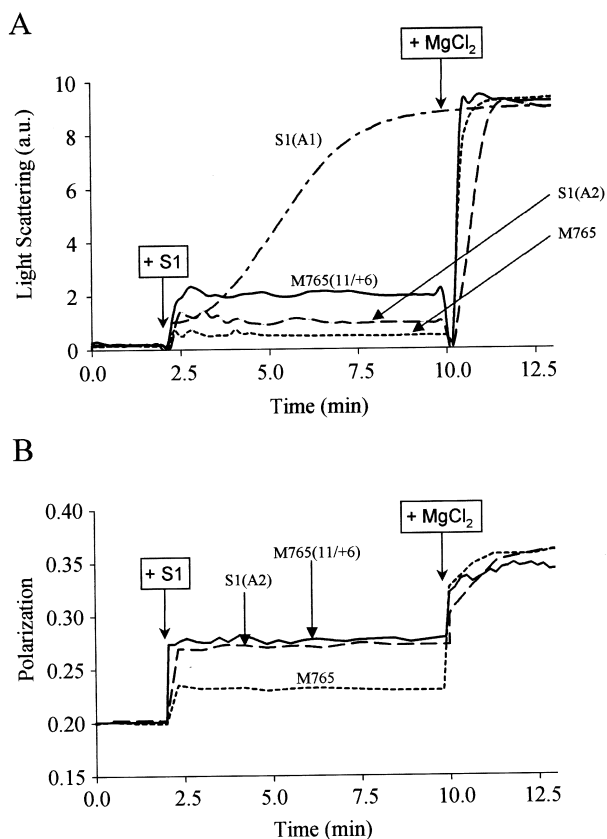


Fig. 2. Effect of M765 constructs on G-actin polymerization. Polymerization of the G-actin-motor domain complexes was monitored by following the changes in light scattering (A) or polarization (B) as described in Materials and methods. A solution of 8 μ M IAEDANS-G-actin in buffer G₅₀ was equilibrated at 25 °C and 8 μ M S1(A₁), S1(A₂), M765 or M765(11/+6) and 2 mM MgCl₂ was added. Maximum dilution of the samples induced by addition of motor domain was less than 10%.

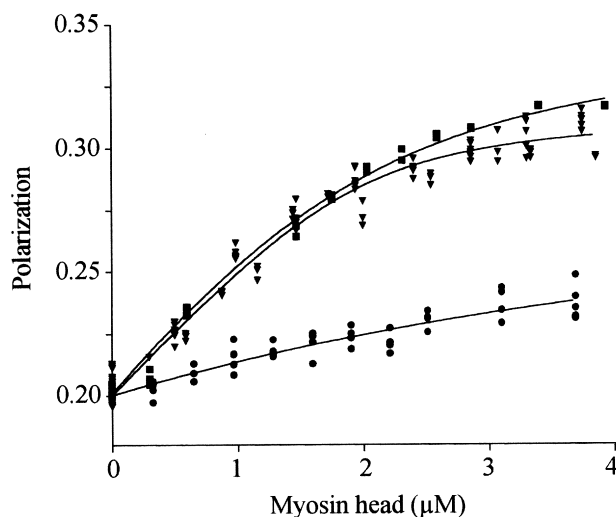


Fig. 3. Interaction of IAEDANS-G-actin to M765 and S1 derivatives. S1(A₂) (∇), M765 (\bullet) or M765(11/+6) (\blacksquare) aliquots were added to a solution of IAEDANS-G-actin (2 μ M) equilibrated at 25 °C in buffer G₅₀ and fluorescence polarization was measured after 2 min incubation as described in Materials and methods. Each point was the average of five measurements and four or five points were recorded for each addition. Data were fitted as described in Materials and methods assuming one binding site and dissociation constants of 0.18, 0.57, and 4.0 μ M for S1(A₂), M765(11/+6) and M765, respectively.

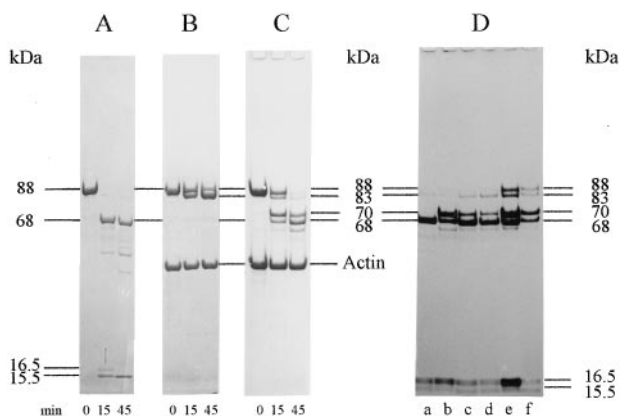


Fig. 4. F-actin and nucleotide effect on trypsin digestion of M765. M765 (20 μM) was cleaved by trypsin for 0, 15, or 45 min in the absence (A) or in the presence of 40 μM F-actin (B and C) without (A and B) or with 20 mM ATP (C). M765 was treated with trypsin for 20 min (D) in the absence (a) or in the presence of ADP (b), ADP.BeF_x (c), ADP.AIF₄⁻ (d), ADP.VO₄³⁻ (e) and ATP (f). All reactions were performed as described in Materials and methods.

In order to determine the affinity constants of the G-actin–S1 complexes, we obtained binding isotherms at 2 μM 1,5-IAEDANS–G-actin by monitoring the enhancement of fluorescence polarization upon addition of S1(A2), M765 or M765(11/+6) in buffer G₅₀ (Fig. 3). The experimental data were fitted to a model which assumes the binding of one S1 per actin monomer [24,37]. The dissociation constants obtained were 0.18, 0.57 and 4.0 μM for the complexes formed with S1(A2), M765(11/+6) and M765, respectively. Measurement of the ATPase activity gave values of 0.3 s⁻¹ for both M765 and M765(11/+6). A value of 0.8 s⁻¹ was obtained for S1(A2) at 25 °C in buffer G. An activity of 0.3 s⁻¹ should lead to the hydrolysis of all the ATP present in buffer G₅₀ by M765 in less than 60 s, i.e. before the second addition of S1 during the binding experiment. Therefore the lower affinity of M765 for G-actin seems to be due to the lower number of charges present in the loop 2 segment of M765 and not to the presence of free ATP.

Characterization of the electrostatic interface between the myosin motor domain and F-actin

Proteolytic digestion of M765. The direct interaction of the N-terminal part of actin with loop 2 of S1 was first demonstrated by the F-actin-induced protection against limited proteolysis [35]. F-actin binding to loop 2 of M765 was first studied by examining the effect of F-actin and nucleotide analogues on the proteolysis pattern of M765. Fig. 4 illustrates the pattern of proteolysis when M765 was treated with trypsin in the absence or in the presence of F-actin and various nucleotide analogues. Trypsin treatment of M765 gave rise to fragments of 68 kDa and 16.5 kDa. The latter was further degraded to a 15.5-kDa band (Fig. 4A). N-terminal sequence analysis revealed that the 68-kDa band was heterogeneous and composed of two fragments with different N-terminal sequences. The first one, which was more abundant at the beginning of the digestion, started at Val17. The second one, which appeared only after extensive cleavage, started at Leu27. The N-terminus of uncleaved M765 could not be sequenced probably because it was blocked. The 16.5-kDa fragment started at Lys623 or at Gly624, whereas the 15.5-kDa fragment always began at Gly624. Only the 16.5-kDa fragment contained a His-Tag as revealed by anti-His-tag

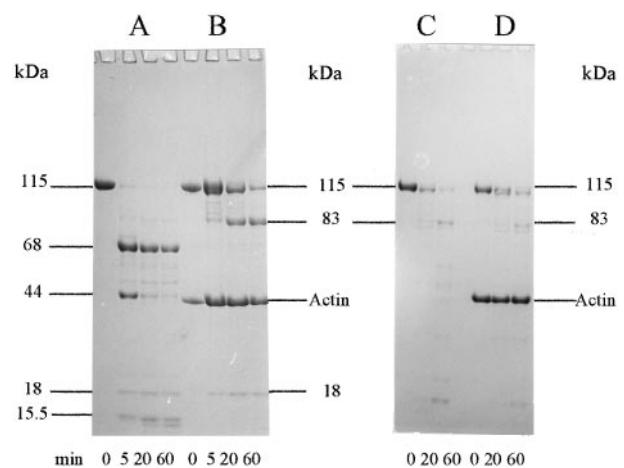


Fig. 5. F-actin effect on trypsin digestion of M761-2R and M761(0/-3)-2R. Twenty micromolar M761-2R (A and B) or M761(0/-3)-2R (C and D) were cleaved by trypsin for 0, 5, 20, or 60 min in the absence (A and C) or in the presence (B and D) of 40 μM F-actin. Samples were analysed by gel electrophoresis as described in Materials and methods.

directed antibodies (not shown). The apparent difference in size between the two fragments (1 kDa) and the size of the His-tag peptide (1.28 kDa) led us to propose a cleavage site around residue Arg761 of M765. The overall results related to trypsin degradation are summarized in Fig. 9.

The presence of F-actin totally protected trypsin proteolysis of M765 at residues Lys622 and Lys623. Only a 83-kDa fragment starting at Val17 (or Leu27 after more extensive treatment) was generated (Fig. 4B). Actin-induced protection was specific because the presence of ATP, which dissociates the actin–S1 complex, again generated the 68-kDa fragment (Fig. 4C). In the presence of both actin and ATP, an additional new band migrating at 70 kDa was produced. This fragment, which also starts at Val17, is a precursor of the 68-kDa fragment. Therefore, it appears that ATP slowed down, whereas actin totally protected the 70–68-kDa transition, i.e. an additional cleavage site located 2 kDa from the C-terminal part of the 70-kDa fragment (Fig. 9). This additional cleavage was also confirmed by the fact that trypsin digestion of M765(8/+4) and M765(11/+6), which possess longer loop 2 sequences, produced a similar 68-kDa band in the absence of actin (data not shown).

The nucleotide-induced protective effect on this 70–68-kDa transition was examined further by using different nucleotide analogues (Fig. 4D). The same degradation pattern was observed in the presence of ADP, ADP.BeF_x, ADP.AIF₄⁻, ADP.VO₄³⁻ or ATP (Fig. 4D, lanes b–f). There seems to be no clear relationship between the extent of proteolysis protection and the nucleotide present in the active site, but protection occurred whenever the active site was occupied by nucleotide. Trypsin proteolysis of M765 in the presence of nucleotide generated an additional band migrating faster, but with a much lower intensity, than the 68-kDa product. Amino acid analysis revealed that this fragment was generated by cleavage at residue Arg70.

The proteolysis patterns obtained with M765 were confirmed with the M761-2R constructs as depicted in Fig. 5. In the absence of actin, two fragments of 68 and 44 kDa were first generated (Fig. 5A). Sequence analysis showed that the 68-kDa fragment was equivalent to the N-terminal 68-kDa fragment obtained with M765 and that the 44-kDa fragment was the C-terminal counterpart beginning at Lys623. Further digestion

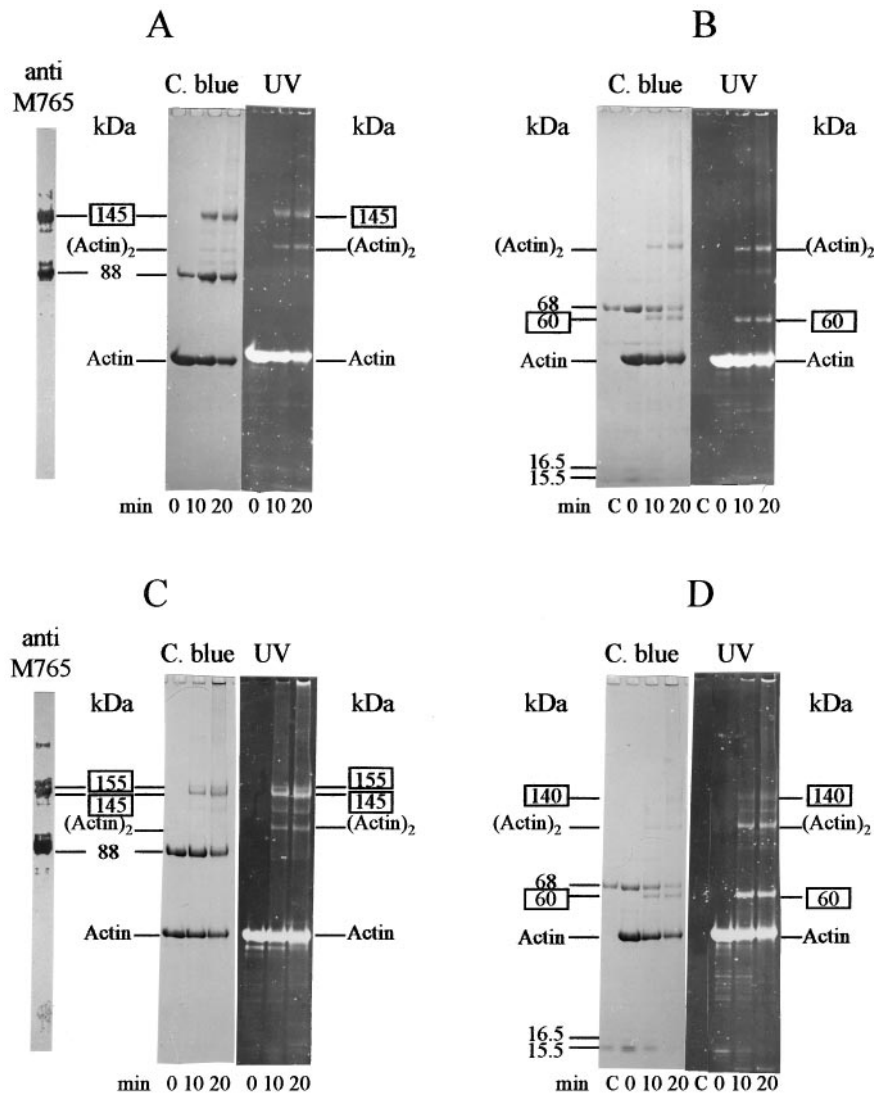


Fig. 6. EDC-induced cross-linking of M765 derivatives to IAEDANS-F-actin. M765 (A and B) or M765(8/+4) (C and D) derivatives were cross-linked to IAEDANS-F-actin before (A and C) or after (B and D) 45 min trypsin digestion as described in Materials and methods. Samples were analysed by SDS/PAGE before (0 min) and after 10 and 20 min reaction (lanes C stand for cleaved M765 and M765(8/+4) derivatives prior to the addition of F-actin). Gels were stained with Coomassie blue or viewed under UV light or immunoblotted with M765 antibodies. Cross-linked products are highlighted by a frame.

of the 44-kDa fragment produced a 15.5-kDa fragment, starting at Gly624, and an 18-kDa fragment starting at Leu840 within the first α -actinin repeat (Figs 5A and 9). In the presence of actin, protection of loop 2 lead to the formation of the 83- and 18-kDa fragments (Fig. 5B).

When M761(0/-3)-2R was digested with trypsin, only the N-terminal 83-kDa fragment (starting at Leu27) and the C-terminal 18-kDa fragment (starting at Leu840) were generated, regardless of the presence of actin (Fig. 5C and D). The 83-kDa fragments obtained in the presence and in the absence of F-actin exhibited similar apparent masses and N-terminal sequences. This result favours the idea that the cleavage at the C-terminal end of the catalytic domain was not altered by F-actin interaction. The F-actin-activated Mg^{2+} -ATPase activity of M765 was unaltered by trypsin treatment (not shown); it is well established that trypsin digestion of S1 leads to a reduction of k_{cat} and an increase of the K_{app} for actin [13,38].

Cross-linking of M765 to F-actin. Carbodiimide-induced cross-linking experiments were used to obtain additional information about the interaction between F-actin and loop 2 in the myosin

motor domain [39,40]. In the presence of NHS, the zero-length cross-linker EDC was found to cross-link the N-terminal segment 1–7 of actin to loop 2 and to loop 559–565 of skeletal muscle myosin [41,42].

When the F-actin–M765 complex was subjected to the EDC-induced reaction, one main cross-linking product was generated, as revealed by SDS/PAGE (Fig. 6A). This covalent 145-kDa adduct contained both actin and M765 as it carried the fluorescence of the IAEDANS moiety attached to actin and reacted with anti-M765 antibodies (Fig. 6A). An additional band containing only actin and migrating with an apparent mass of 120 kDa was identified as actin dimer (Fig. 6A, [42]). Cross-linking experiments performed under identical conditions on a complex between F-actin and trypsin-cleaved (68–16.5/15.5 kDa)-M765 derivative gave rise to two products positive in actin (Fig. 6B). One product, migrating at 120 kDa, consists of actin dimer and the second product of 60 kDa most likely contains 1 mole of actin covalently bound to the 16.5-kDa C-terminal fragment of M765. This last conclusion is based on the following results: firstly, when the cross-linking reaction was performed after extensive trypsin treatment, i.e. with only the

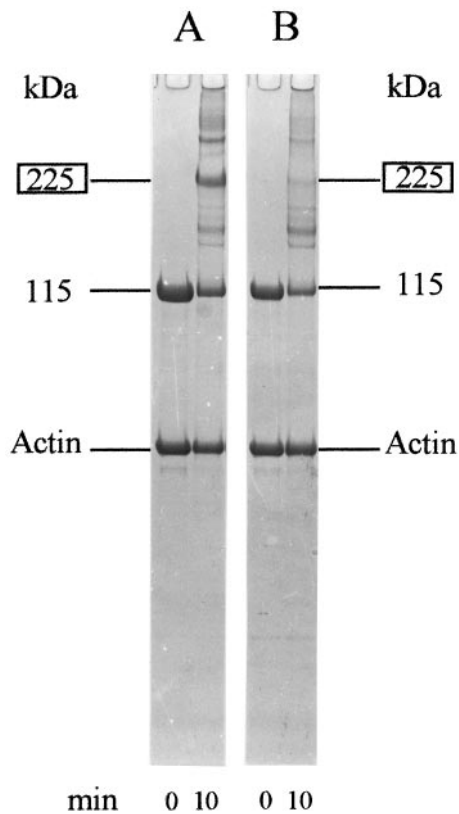


Fig. 7. EDC-induced cross-linking of F-actin to M761-2R and M761(0/-3)-2R constructs. Fifteen micromolar M761-2R (A) or M761(0/-3)-2R (B) was mixed with 45 μM F-actin in cross-linking buffer. The cross-linking reactions were performed as described in Materials and methods and the samples were analysed by SDS/PAGE after 0 and 10 min reaction. Cross-linked products are highlighted by a frame.

68–15.5-kDa adduct, the 60-kDa band was lost (data not shown) and secondly, the N-terminal sequence of the cross-linked 60-kDa product was found to start at Gly624, suggesting that the missing N-terminal residue of the 16.5-kDa fragment, Lys623, is directly implicated in the cross-linking to actin.

When cross-linking experiments were performed with F-actin bound to M765(8/+4), an additional cross-linking product of 155 kDa was obtained (Fig. 6C). This product contained both actin (fluorescent band) and M765 (immuno-reactive with anti-M765). The yield of the 155-kDa-product was always very low as compared with the main covalent product of 145 kDa. In the case of the 155-kDa product, cross-linking most probably occurred between actin and one or several of the additional lysine residues present in loop 2 of M765(8/+4) (Fig. 1). When the reaction was performed with the tryptic derivative of M765(8/+4), a 60-kDa product and a very faint 140-kDa band positive for fluorescent actin were obtained (Fig. 6D). The 60-kDa product was also obtained with M765. The exact composition of the 140-kDa band is still unclear; however, as it is only a minor product, it may result from cross-linking between actin and the 70-kDa peptide that is the product of incomplete trypsin cleavage. Very similar cross-linking patterns were obtained with M765(11/+6) (data not shown).

Cross-linking reactions performed on the F-actin–M761–2R complex led to a single product of 225 kDa (Fig. 7A). Removal of the two lysine residues of loop 2 such as in the M761(0/+3)-2R construct resulted in the complete loss of the

225-kDa product (Fig. 7B). The slight decrease in the amount of protein observed during the reaction was probably due to nonspecific cross-linking products migrating at the top of the gel. This result is again consistent with cross-linking taking place between actin and the lysine residues of loop 2.

To identify the cross-linking sites within actin, we subjected the isolated and depolymerized 145- and 155-kDa actin–M765 complexes to proteolysis by thrombin, which cleaves monomeric actin at residues 28, 39, and 113 [43,44] but does not attack M765 (Fig. 8). Thrombin digestion of the 145-kDa (actin–M765) and of the 155-kDa [actin–M765(8/+4)] products generated one band of 90 kDa (Fig. 8 IA, lane c) and two bands of 90 and 96 kDa (Fig. 8 IB, lane c), respectively. All three proteolysis products contained M765 as revealed by immunostaining with anti-M765 antibodies (Fig. 8E and F, lanes c), but none of them included the fluorescent C-terminal actin fragments (carrying the fluorescent label on residue Cys374; Fig. 8 IC and D, lanes c). In addition there was no fluorescent intermediate generated during the cleavage reaction. Therefore, none of the cross-linked products contained either actin segment 40–374 or 114–374 (Fig. 8 II). As actin peptide 29–39 does not contain the acidic residues capable of reacting with EDC, it is more likely that the 90-kDa product contained M765 bound to actin peptide 1–28. Similarly, the cross-linking of the same actin peptide 1–28 to skeletal muscle myosin S1 led to a product of 100 kDa which migrates with a slightly higher apparent mass than the 95-kDa S1 heavy chain fragment [45,46]. The 96-kDa product probably results from cross-linking of the additional lysine residues of M765(8/+4) to acidic residues in the same actin peptide 1–28.

Actin-activated ATPase activities

We first compared the effect of G- and F-actin on the Mg^{2+} -ATPase activities of M765 and S1 derivatives. In buffer G, the Mg^{2+} -ATPase activity was very similar (in the order of 0.05 s^{-1}) for S1(A2), M765 and M761(11/+6) (Table 1). In the presence of G-actin, the Mg^{2+} -ATPase activities of S1(A2) and M761(11/+6) were increased 2.4- and 3.3-fold, as compared with the 57- and 36-fold activation observed in the presence of F-actin, respectively. On the other hand, the activity of M765 remained unchanged in the presence of G-actin and was activated only by a factor of 2.8 in the presence of F-actin. This last result is in good agreement with the poor binding of M765 to G-actin and the low efficiency of the F-actin induced activation of M765 (see below).

Recently, Furch *et al.* [16] reported how the number of positively-charged residues in loop 2 affects the parameters of the actin-activated ATPase activity of M765. In these experiments, the simple addition of four charges in the primary sequence of loop 2 produced a 12-fold reduction of the K_{app} for actin and a > 40-fold increase in the catalytic efficiency of the reaction ($k_{\text{cat}}/K_{\text{app}}$). The measurements of the ATPase activity of the covalent (cross-linked) complexes also revealed a lower activity for the F-actin–M765 ($1.58 \pm 0.22 \text{ s}^{-1}$) than for the F-actin–M765(8/+4) ($4.28 \pm 0.33 \text{ s}^{-1}$) complex. Interestingly, the value obtained with the M765(8/+4) construct was of the same magnitude than the values obtained when actin was cross-linked with either S1(A1) ($4.75 \pm 0.19 \text{ s}^{-1}$) or S1(A2) ($4.61 \pm 0.10 \text{ s}^{-1}$). In all cases, the similarity of k_{cat} obtained for cross-linked and reversible complexes shows the specificity of the cross-linking reaction which always results in fully active complexes.

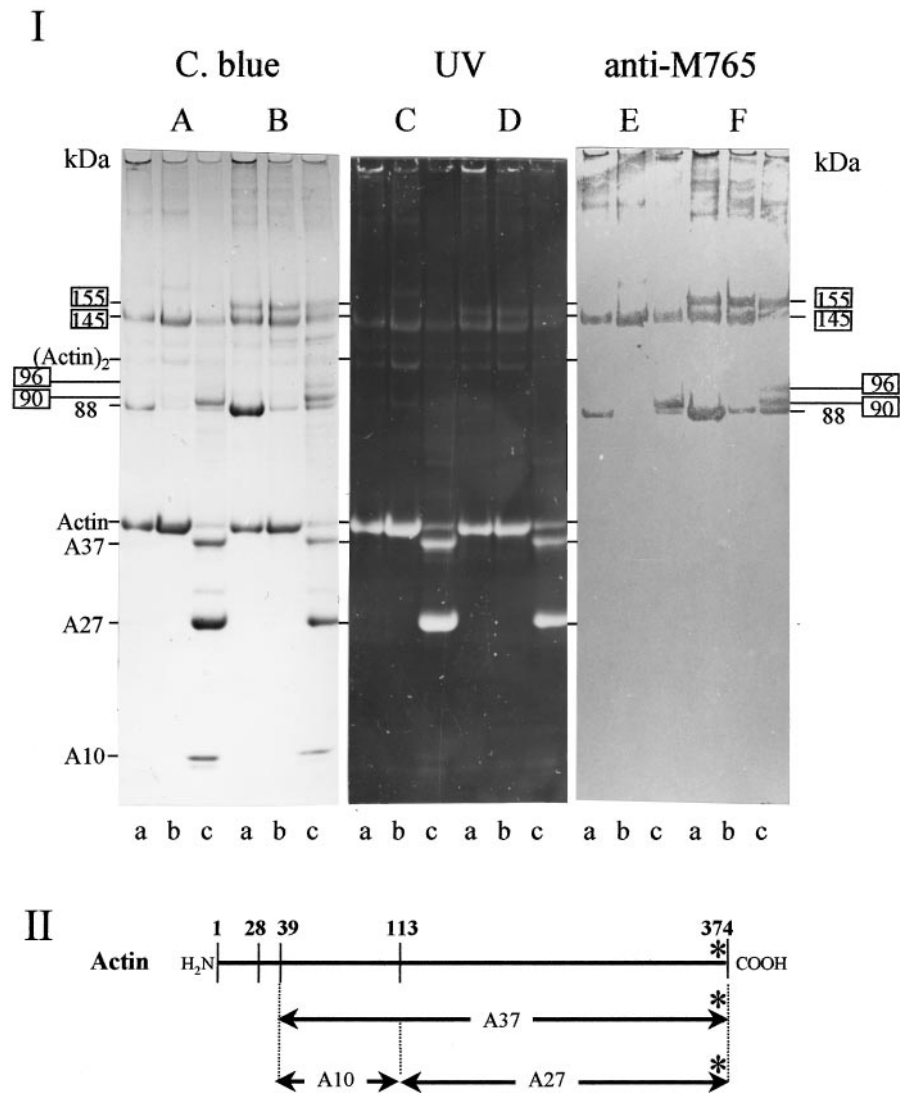


Fig. 8. Thrombin degradation of the covalent actin–S1 adducts. Panel I, M765 (A, C, E) or M765(8/+4) (B, D, F) were cross-linked to IAEDANS–F-actin and subjected to thrombin cleavage as described in Materials and methods. Cross-linked actin–S1 complexes (lanes a) were treated with KI to remove uncross-linked S1 (lanes b) and subsequently depolymerized and digested by thrombin for 20 min (lanes c). Gels were stained with Coomassie blue (A and B), viewed under UV light (C and D) or immunoblotted with M765 antibodies (E and F). A37, A27 and A10 are thrombin peptides of actin 40–375, 114–375 and 40–113, respectively. Cross-linked products are highlighted by a frame. Panel II, schematic representation of the thrombin sites and the corresponding peptic fragments along the actin sequence. Residue Cys374 carrying the fluorescent probe is marked (★).

DISCUSSION

This work provides experimental evidence for the direct implication of loop 2 of nonmuscle and muscle myosin II in both the binding to G-actin and to F-actin. Table 2 summarizes the overall results obtained in this study.

Table 1. Comparative effect of G- and F-actin on the Mg^{2+} -ATPase activities of M765 and S1 derivatives.

| Motor domain | Mg^{2+} -ATPase activities (s^{-1}) ^a | | |
|--------------|--|--------------------------------|--------------------------------|
| | Alone | With G-actin | With F-actin |
| S1(A2) | 0.05 ± 0.02 | 0.12 ± 0.01 (2.4) ^b | 2.88 ± 0.02 (57) ^b |
| M765 | 0.05 ± 0.03 | 0.05 ± 0.02 (1) ^b | 0.14 ± 0.01 (2.8) ^b |
| M761(11/+6) | 0.06 ± 0.03 | 0.20 ± 0.04 (3.3) ^b | 2.17 ± 0.02 (36) ^b |

^aThe Mg^{2+} -ATPase activities were measured at 25 °C as described [35]. Experimental conditions: 1 μ M motor domain in the absence or in the presence of 5 μ M G- or F-actin in 5 mM Hepes, 0.1 mM $CaCl_2$, 0.15 mM EGTA, 2 mM MgATP, PH8.0. ^bActivation factor.

Interaction between G-actin and the myosin motor domains

D. discoideum motor domain binds to G-actin with a very low affinity as compared with skeletal muscle S1(A2). This difference could be accounted for by variations in the primary sequences of the two proteins or simply by the presence, in muscle myosin S1, of the regulatory domain (associated with the A2 light chain). Due to the low affinity constant of M765, no attempt was made to determine the stoichiometry of the complex formed between G-actin and the M765 constructs. However, it is likely that the *D. discoideum* motor domain forms a 1 to 1 complex with G-actin as previously found for muscle myosin S1 under comparable conditions [23,24,37,47,48]. Increasing the number of positive charges in loop 2 of M765 increases its affinity for G-actin to the level of S1(A2). This result strongly suggests that the number of charges present in this surface loop drives the strength of the interaction between G-actin and myosin. A similar conclusion was previously derived from experiments with skeletal muscle myosin which

Table 2. Summary of the actin binding properties of the motor domain constructs of skeletal muscle and *D. discoideum* myosin.

| Motor domain construct | G-actin binding | | F-actin binding | | | k_{cat} of X-linked complexes (s^{-1}) | k_{cat}/K_{app} ($\times 10^{-2} \cdot M^{-1} \cdot s^{-1}$) ^c |
|------------------------|-------------------|-----------------------------|-----------------------------------|---------------------|---------------------------|--|---|
| | K_d (μM) | Polymerization ^a | Protection of loop 2 ^b | X-linking to loop 2 | X-linking to loop 559–565 | | |
| S1 | 0.18 | \pm^d | + | + | + | 4.67 ^e | 2.5 ^f |
| M765 | 4.0 | – | + | + | – | 1.58 | 0.25 ^g |
| M765(8/+4) | n.d. | – | + | ++ ^h | – | 4.28 | 10.2 ^g |
| M765(11/+6) | 0.57 | – | + | ++ ^h | – | n.d. | n.d. |
| M761-2R | n.d. ⁱ | n.d. ⁱ | + | + | – | n.d. | n.d. |
| M761(0/-3)-2R | n.d. ⁱ | n.d. ⁱ | n.d. ^j | – | – | n.d. | n.d. |

^aG-actin polymerization induced by myosin motor domain in buffer G₅₀. ^bProtection of loop 2 against trypsin degradation. ^cValues for k_{cat} and K_{app} were calculated for the reversible complexes from fitting the ATPase activities obtained at various actin concentrations to the Michaelis–Menten equation. ^dS1(A1) induces actin polymerization whereas S1(A2) does not. ^eAveraged values for cross-linked complexes obtained with the two isoforms. ^fAveraged value calculated from k_{cat}/K_{app} ($s^{-1}/\mu M$) of 5.0/12.9 and 4.8/38.9 obtained for the reversible F-actin–S1(A2) and F-actin–S1(A1) complexes. ^gFrom [16]. ^hAdditional cross-linking occurs between mutated loop 2 and actin subdomain 1. ⁱ2R-containing constructs cannot be used because G-actin interacts nonspecifically with 2R segment in G-buffer. ^jTrypsin does not attack loop 2 of this construct.

showed that blocking the charges of loop 2 with a ‘complementary’ peptide inhibits S1 binding to G-actin [36]. Furthermore, the fact that the dissociation constant of G-actin for S1(A2) is threefold lower than for M765(11/+6) can be explained by differences in the number and distribution of charged residues in the loop 2 region (Fig. 1). Note that in both cases, G-actin is unable to activate the Mg²⁺-ATPase activity of the motor domain as described previously only for muscle myosin derivatives [34].

Similar to S1(A2), the ability of M765 to induce polymerization of G-actin is poor and the salt-induced polymerization of actin is accelerated in the presence of both proteins. The addition of six positive charges in loop 2 of M765(11/+6) has no effect on these properties. These data clearly show that loop 2 is not involved in the myosin-induced polymerization of G-actin.

Interaction between F-actin and the loop 2 segment of the myosin motor domains

Proteolysis experiments. The loop 1 and loop 2 segments of skeletal, cardiac and smooth muscle myosin S1 have been known for a long time to be susceptible to hydrolytic cleavage by a wide variety of proteases, giving rise to three proteolytic fragments of 25, 50 and 20 kDa [49–53]. Proteolysis experiments revealed that M765 is cleaved by trypsin at three distinct sites as summarized in Fig. 9: near the N-terminus, at Lys16 and Lys26, in the vicinity of loop 2 segment, at Lys622 and Lys623, and close to the C-terminus, near to Arg761. Except for the cleavage at the two extremities, the main difference between nonmuscle and skeletal muscle myosin II is the resistance of the loop 1 region of the *D. discoideum* motor domain to proteolytic

degradation. None of the three proteases that were additionally tested (chymotrypsin, V8-protease and Arg-C endoproteinase), attacked either loop 1 or loop 2. Proteolytic resistance of loop 1 was previously described for other nonmuscle myosin II isoforms such as *Acanthamoeba castellanii* myosin II [54] and brain myosin II [55]. In the case of *D. discoideum* M765, this resistance may not only be due to the absence of charged residues but also to the shortness of the loop, making it less flexible and less accessible to proteases [14,56].

Additional information can be derived from the proteolytic pattern obtained in the presence of actin and nucleotide analogues. Actin-mediated protection of loop 2 against proteolytic degradation has been observed for all myosins studied, so far ([39,44,57,58], this work). Our finding that degradation of M765 by trypsin does not affect the ATPase activities of M765 is different from the result obtained with skeletal muscle myosin S1, as trypsinolysis of S1 strongly reduces its actin-activated ATPase activity. A single cleavage site in M765 loop 2, versus multiple sites in S1 loop 2, may eventually explain this difference.

The presence of nucleotide has a strong modulating effect on the proteolytic cleavage pattern of muscle myosin. Additionally, modifications in the rates of cleavage of loop 1 and loop 2 are observed [12,59–61]. The most important change detected with nonmuscle myosin II, regardless of the nature of the nucleotide, is the protection of a cleavage site located 2 kDa from loop 2 inside the 70-kDa NH₂-terminal fragment.

Cross-linking experiments. The second experimental argument in favour of actin binding to myosin loop 2 arises from the carbodiimide-induced cross-linking experiments. All myosins studied so far can be cross-linked to F-actin by EDC [39,62,63]. In good agreement with the image reconstruction of the

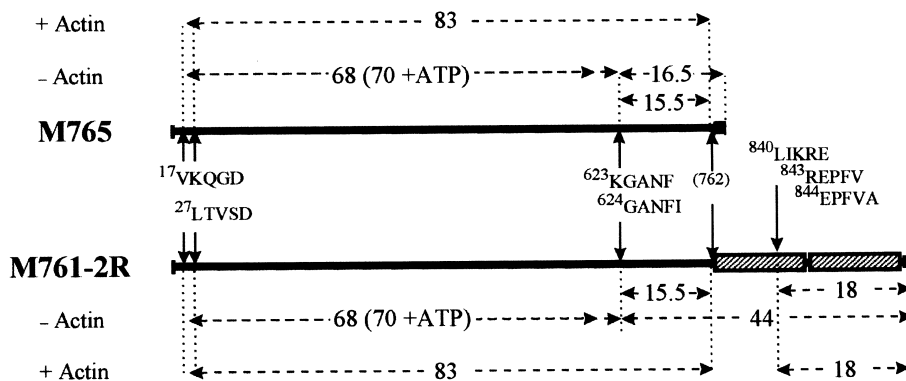


Fig. 9. Schematic diagram illustrating the localization of trypsin cleavage sites along M765 constructs. Trypsin sites were deduced from N-terminal sequence analysis of the proteolytic fragments as described in Materials and methods. Numbers are apparent M_r in kDa.

rigor-complex formed by F-actin and the *D. discoideum* motor domain [8], M765 is cross-linked to the NH₂ terminal part of actin subdomain 1. Two experimental results lead to the identification of the cross-linking site within the loop 2 segment of myosin. First, the COOH-terminal tryptic fragment of M765 obtained after mild trypsin treatment (starting at Lys623) but not that resulting from a more extensive trypsin digestion (starting at Gly624) is cross-linked to F-actin. Second, construct M761(0/-3)-2R, which does not contain lysine residues in the loop 2 segment, binds to F-actin as judged by co-sedimentation experiments performed in rigor conditions but cannot be cross-linked to actin by EDC treatment. Other cross-linking reagents, such as glutaraldehyde or dimethylsuberimidate known to cross-link skeletal myosin loop 2 to F-actin [64,65] do not induce significant cross-linking of actin to *D. discoideum* myosin constructs (data not shown).

When the cross-linking reaction is performed with the G-actin–M765 complex under nonpolymerizing conditions [23], a single cross-linking product is obtained that migrates with a molecular mass of 145 kDa (data not shown). The size of this product, which is identical to that described for the F-actin–M765 complex, confirms the involvement of loop 2 in the interface between M765 and G-actin.

Cross-linking experiments carried out with M765 mutants that contain a longer, positively-charged loop 2 sequence revealed a secondary contact with the negative charged region of actin subdomain 1. This secondary contact can be related to the higher k_{cat} values obtained for both the reversible and the cross-linked complexes and it may cause the increased catalytic efficiency observed with constructs M765(8/+4) and M765(11/+6) ([16]; Table 2). Therefore, it is likely that the dramatic decrease of K_{app} previously reported by Furch *et al.* [16] with these mutants is due to a better interaction of the loop 2 segment with its natural binding site on actin and not to additional nonspecific contacts.

No cross-linking products corresponding to the linkage between F-actin and the loop 559–565 of the *D. discoideum* motor domain could be assigned. As a consequence, the product containing the motor domain covalently bound to two actin molecules via loop 613–623 and loop 559–565 [66] is also absent in the cross-linking mixture. In the case of skeletal and cardiac muscle myosin, it was proposed that loop 559–565 interacts with the negatively-charged residues of the lower actin monomer predominantly when the actin filament is not saturated by myosin (with an actin/motor domain ratio higher than 2; [42,66,67]). Moreover this interaction was recently found to be predominant in the weak binding interface [17]. The lack of cross-linking products involving the loop 559–565 of all M765 constructs can easily be related to the absence of positively-charged residues in this region of *D. discoideum* myosin [6]. Similarly, the motor domain of smooth muscle myosin does not cross-link via this loop [62]. Whether the interaction of actin with myosin loop 559–565 is a specific property of striated muscle myosins (i.e. for skeletal and cardiac muscle) or occurs in other forms of myosin as well remains to be elucidated.

Finally, the presence of a regulatory domain-like structure, such as the two α -actinin repeats present in the M761-2R constructs, does not affect the results obtained with the M765 mutants. This finding confirms that the regulatory domain of the motor domain is not needed for normal actin binding and actin-activated ATPase activity [16].

In conclusion, the carboxylate groups of actin subdomain 1 form ionic contacts with the positively-charged residues present in loop 2 of both muscle and nonmuscle myosin II. The number of ionic contacts involved in this interface is an essential

parameter that tunes the catalytic efficiency of the motor domain and the stability of the actin–myosin complex in both weak and strong binding states. They also have a critical role in the binding of myosin to G-actin but in contrast, they do not seem to be directly involved in the polymerization of G-actin induced by myosin derivatives. Other ionic contacts, implicating myosin region 559–565 and an adjacent actin, seems to be specific for striated muscle myosin. Their exact role during the catalytic activity of this type of myosin is now under investigation.

ACKNOWLEDGEMENTS

We thank S. Zimmermann for excellent technical assistance and the generation of plasmid constructs. D.J.M., M.F., R.B. and M.L.W.K. thank K. C. Holmes for continuous support and encouragement.

This work was supported by the Centre National de la Recherche Scientifique, the Association Française contre les myopathies and the Max-Planck Society.

REFERENCES

1. Fisher, A.J., Smith, C.A., Thoden, J., Smith, R., Sutoh, K., Holden, H.M. & Rayment, I. (1995). Structural studies of myosin-nucleotide complexes: a revised model for the molecular basis of muscle contraction. *Biophys. J.* **68**, 19S–28S.
2. Marston, S.B. & Taylor, E.W. (1980) Comparison of the myosin and actomyosin ATPase mechanisms of the four types of vertebrate muscles. *J. Mol. Biol.* **139**, 573–600.
3. Ritchie, M.D., Geeves, M., Woodward, S.K.A. & Manstein, D.J. (1993) Kinetic characterization of a cytoplasmic myosin motor domain expressed in *Dictyostelium discoideum*. *Proc. Natl Acad. Sci. USA* **90**, 8619–8623.
4. Ostap, E.M. & Pollard, T.D. (1996) Biochemical kinetic characterization of the *Acanthamoeba* myosin-I ATPase. *J. Cell Biol.* **132**, 1053–1060.
5. Nascimento, A.A.C., Cheney, R.E., Tauhata, S.B.F., Larson, R.E. & Mooseker, M.S. (1996) Enzymatic characterization and functional domain mapping of brain myosin-V. *J. Biol. Chem.* **271**, 17561–17569.
6. Sellers, J.R. & Goodson, H.V. (1995) Motor proteins 2: myosin. *Protein Profile* **2**, 1323–1423.
7. Rayment, I., Holden, H.M., Whittaker, M., Yohn, C.B., Lorenz, M., Holmes, K.C. & Milligan, R.A. (1993) Structure of the actin–myosin complex and its implications for muscle contraction. *Science* **261**, 58–61.
8. Schröder, R.R., Manstein, D.J., Jahn, W., Holden, H., Rayment, I., Holmes, K.C. & Spudich, J.A. (1993) Three-dimensional atomic model of F-actin decorated with *Dictyostelium* myosin S1. *Nature* **364**, 171–174.
9. Mendelson, R. & Morris, E.P. (1997) The structure of the acto-myosin subfragment 1 complex: results of searches using data from electron microscopy and X-ray crystallography. *Proc. Natl Acad. Sci. USA* **94**, 8533–8538.
10. Chaussepied, P. & Morales, F. (1988) Modifying preselected sites on proteins: The stretch of residues 633–642 of the myosin heavy chain is part of the actin-binding site. *Proc. Natl Acad. Sci. USA* **85**, 7471–7475.
11. Chaussepied, P. (1989) Interaction between stretch of residues 633–642 (actin binding site) and nucleotide binding site on skeletal myosin subfragment 1 heavy chain. *Biochemistry* **28**, 9123–9128.
12. Yamamoto, K. (1989) ATP-induced structural change in myosin subfragment-1 revealed by the location of protease cleavage sites on the primary structure. *J. Mol. Biol.* **209**, 703–709.
13. Bobkov, A.A., Bobkova, E.A., Lin, S.H. & Reisler, E. (1996) The role of surface loops (residues 204–216 and 627–646) in the motor function of the myosin head. *Proc. Natl Acad. Sci. USA* **93**, 2285–2289.
14. Uyeda, T.Q.P., Ruppel, K.M. & Spudich, J.A. (1994) Enzymatic activities correlate with chimaeric substitutions at the actin-binding face of myosin. *Nature* **368**, 567–569.
15. Rovner, A.S., Freyzon, Y., & Trybus, K.M. (1995) Chimeric substitutions of the actin-binding loop activate dephosphorylated but not

- phosphorylated smooth muscle heavy meromyosin. *J. Biol. Chem.* **270**, 30260–30263.
16. Furch, M., Geeves, M.A. & Manstein, D.J. (1998) Modulation of actin affinity and actomyosin ATPase by charge changes in the myosin motor domain. *Biochemistry* **37**, 6317–6326.
 17. Van Dijk, J., Fernandez, C. & Chaussepied, P. (1998) Effect of ATP analogues on the actin–myosin interface. *Biochemistry* **37**, 8385–8394.
 18. Kurzawa, S.E., Manstein, D.J. & Geeves, M.A. (1997) *Dictyostelium discoideum* myosin II: characterization of functional myosin motor fragments. *Biochemistry* **36**, 317–323.
 19. Anson, M., Geeves, M.A., Kursawa, S.E. & Manstein, D.J. (1996) Myosin motors with artificial lever arms. *EMBO J.* **15**, 6069–6074.
 20. Wagner, P.D. & Weeds, A.G. (1979) Determination of the association of myosin subfragment 1 with actin in the presence of ATP. *Biochemistry* **18**, 2260–2266.
 21. Lowey, S., Waller, G.S., Trybus, K. & M. (1993) Function of skeletal muscle myosin heavy and light chain isoforms by an *in vitro* motility assay. *J. Biol. Chem.* **268**, 20414–20418.
 22. Lowey, S., Waller, G.S. & Trybus, K.M. (1993) Skeletal muscle myosin light chains are essential for physiological speeds of shortening. *Nature* **365**, 454–456.
 23. Chaussepied, P. & Kasprzak, A.A. (1989) Isolation and characterization of the G-actin-myosin head complex. *Nature* **342**, 950–953.
 24. Lheureux, K., Forné, T. & Chaussepied, P. (1993) Interaction and polymerization of the G-actin-myosin head complex: effect of DNase I. *Biochemistry* **32**, 10005–10014.
 25. Offer, G., Moos, C. & Starr, R. (1973) A new protein of the thick filaments of vertebrate skeletal myofibrils. Extractions, purification and characterization. *J. Mol. Biol.* **74**, 653–676.
 26. Weeds, A.G. & Taylor, R.S. (1975) Separation of subfragment-1 isoenzymes from rabbit skeletal muscle myosin. *Nature* **257**, 54–56.
 27. Eisenberg, E. & Kielley, W.W. (1974) Troponin–tropomyosin complex. Column chromatographic separation and activity of the three active troponin components with and without tropomyosin present. *J. Biol. Chem.* **249**, 4742–4748.
 28. Manstein, D.J. & Hunt, D.M. (1995) Overexpression of myosin motor domain in *Dictyostelium*: screening of transformants and purification of the affinity tagged protein. *J. Muscle Res. Cell Motil.* **16**, 325–332.
 29. Bradford, M.M. (1976) A rapid and sensitive method for the quantitation of microgram quantities of protein utilizing the principle of protein-dye binding. *Anal. Biochem.* **72**, 248–254.
 30. Goodno, C.C. (1982) Myosin active-site trapping with vanadate ion. *Methods Enzymol.* **85**, 116–123.
 31. Laemmli, U.K. (1970) Cleavage of structural proteins during the assembly of the head of bacteriophage T4. *Nature* **227**, 680–685.
 32. Bonafé, N., Chaussepied, P., Capony, J.P., Derancourt, J. & Kassab, R. (1993) Photochemical cross-linking of the skeletal myosin head heavy chain to actin subdomain-1 at Arg95 and Arg28. *Eur. J. Biochem.* **213**, 1243–1254.
 33. Mandelkow, E.M. & Mandelkow, E. (1973) Fluorimetric studies on the influence of metal ions and chelators on the interaction between myosin and ATP. *FEBS Lett.* **33**, 161–166.
 34. Lheureux, K. & Chaussepied, P. (1995) Comparative studies of the monomeric and filamentous actin-myosin head complexes. *Biochemistry* **34**, 11435–11444.
 35. Mornet, D., Bertrand, R., Pantel, P., Audemard, E. & Kassab, R. (1981) Proteolytic approach to structure and function of actin recognition site in myosin heads. *Biochemistry* **20**, 2110–2120.
 36. Chaussepied, P. & Kasprzak, A.A. (1989) Change in the actin-myosin subfragment 1 interaction during actin polymerization. *J. Biol. Chem.* **264**, 20752–20759.
 37. Kasprzak, A.A. (1993) Myosin subfragment 1 inhibits dissociation of nucleotide and calcium from G-actin. *J. Biol. Chem.* **268**, 13261–13266.
 38. Botts, J., Muhlrud, A., Takashi, R. & Morales, M.F. (1982) Effects of tryptic digestion on myosin subfragment 1 and its actin-activated adenosinetriphosphatase. *Biochemistry* **21**, 6903–6905.
 39. Mornet, D., Bertrand, R., Pantel, P., Audemard, E. & Kassab, R. (1981) Structure of the actin–myosin interface. *Nature* **292**, 301–306.
 40. Sutoh, K. (1982) Identification of myosin-binding sites on the actin sequence. *Biochemistry* **21**, 3654–3661.
 41. Andreeva, A.L., Andreev, O.A. & Borejdo, J. (1993) Structure of the 265-kilodalton complex formed upon EDC cross-linking of subfragment 1 to F-actin. *Biochemistry* **32**, 13956–13960.
 42. Bonafé, N. & Chaussepied, P. (1995) A single myosin head can be cross-linked to the N termini of two adjacent actin monomers. *Biophys. J.* **68**, 35–43.
 43. Muszbek, L., Gladner, J.A. & Laki, K. (1975) The fragmentation of actin by thrombin. Isolation and characterization of the split products. *Arch. Biochem. Biophys.* **167**, 99–103.
 44. Bertrand, R., Chaussepied, P., Audemard, E. & Kassab, R. (1989) Functional characterization of skeletal F-actin labeled on the NH₂-terminal segment of residues 1–28. *Eur. J. Biochem.* **181**, 747–754.
 45. Bertrand, R., Chaussepied, P., Kassab, R., Boyer, M., Roustan, C. & Benyamin, Y. (1988) Cross-linking of the skeletal myosin subfragment 1 heavy chain to the N-terminal actin segment of residues 40–113. *Biochemistry* **27**, 5728–5736.
 46. Elzinga, M. (1987) Carboxyl group reactivity in action. In *Methods in Protein Science Analysis*. (Walsh, J.E., ed.), pp. 615–623. The Human Press, Totowa, NJ, USA.
 47. Chen, T. & Reisler, E. (1991) Interactions of myosin subfragment 1 isozymes with G-actin. *Biochemistry* **30**, 4546–4552.
 48. Miller, L., Phillips, M. & Reisler, E. (1988) Polymerization of G-actin by myosin subfragment 1. *J. Biol. Chem.* **263**, 1996–2002.
 49. Balint, M., Wolf, I., Tarcsafalvi, A., Gergely, J. & Streter, F.A. (1978) Location of SH-1 and SH-2 in the heavy chain segment of heavy meromyosin. *Arch. Biochem. Biophys.* **190**, 793–799.
 50. Marianne-Pépin, T., Mornet, D., Audemard, E. & Kassab, R. (1983) Structural and actin-binding properties of the trypsin-produced HMM and S1 from gizzard smooth muscle myosin. *FEBS Lett.* **159**, 211–216.
 51. Bonet, A., Mornet, D., Audemard, E., Derancourt, J., Bertrand, R. & Kassab, R. (1987) Comparative structure of the protease-sensitive regions of the subfragment-1 heavy chain from smooth and skeletal myosins. *J. Biol. Chem.* **262**, 16524–16530.
 52. Lompré, A.M., Han, K.K., Bouveret, P., Richard, C. & Schwartz, K. (1984) Comparison of the tryptic digestion pattern of subfragments 1 from V1 and V3 rat cardiac isomyosins. *Eur. J. Biochem.* **139**, 459–465.
 53. Mornet, D., Ue, K. & Morales, M.F. (1984) Proteolysis and the domain organization of myosin subfragment 1. *Proc. Natl Acad. Sci. USA* **81**, 736–739.
 54. Kuznicki, J., Atkinson, M.A. & Korn, E.D. (1984) Effects of limited tryptic cleavage on the physical and enzymatic properties of myosin II from *Acanthamoeba castellanii*. *J. Biol. Chem.* **259**, 9308–9313.
 55. Barylko, B., Tooth, P. & Kendrick-Jones, J. (1986) Proteolytic fragmentation of brain myosin and localisation of the heavy-chain phosphorylation site. *Eur. J. Biochem.* **158**, 271–282.
 56. Murphy, C.T. & Spudich, J.A. (1998) *Dictyostelium* myosin 25–50K loop substitutions specifically affect ADP release rates. *Biochemistry* **37**, 6738–6744.
 57. Chaussepied, P., Bertrand, R., Audemard, E., Pantel, P., Derancourt, J. & Kassab, R. (1983) Selective cleavage of the connector segments within the myosin-S1 heavy chain by staphylococcal protease. *FEBS Lett* **161**, 84–88.
 58. Brzeska, H., Lynch, T.J. & Korn, E.D. (1989) The effect of actin and phosphorylation on the tryptic cleavage pattern of *Acanthamoeba* myosin IA. *J. Biol. Chem.* **264**, 10243–10250.
 59. Applegate, D. & Reisler, E. (1984) Nucleotide-induced changes in the proteolytically sensitive regions of myosin subfragment 1. *Biochemistry* **23**, 4779–4784.
 60. Mornet, D., Pantel, P., Audemard, E., Derancourt, J. & Kassab, R. (1985) Molecular movements promoted by metal nucleotides in the heavy-chain regions of myosin heads from skeletal muscle. *J. Mol. Biol.* **183**, 479–489.
 61. Redowicz, M.J., Szilagyi, L. & Strzelecka-Golaszewska, H. (1987) Conformational transitions in the myosin head induced by temperature, nucleotide and actin. Studies on subfragment-1 of myosins from rabbit and frog fast skeletal muscle with a limited proteolysis method. *Eur. J. Biochem.* **165**, 353–362.

62. Marianne-Pépin, T., Mornet, D., Bertrand, R., Labbé, J.P. & Kassab, R. (1985) Interaction of the heavy chain of gizzard myosin heads with skeletal F-actin. *Biochemistry* **24**, 3024–3029.
63. Labbé, J.P., Chaussepied, P., Derancourt, J. & Kassab, R. (1988) Interaction of the heavy chain of scallop myosin heads with skeletal F-actin. *Biochemistry* **27**, 5914–5922.
64. Labbé, J.P., Mornet, D., Roseau, G. & Kassab, R. (1982) Cross-linking of F-actin to skeletal muscle myosin subfragment 1 with Bis (imido esters): further evidence for the interaction of myosin head heavy chain with an actin dimer. *Biochemistry* **21**, 6897–6902.
65. Bonafé, N., Mathieu, M., Kassab, R. & Chaussepied, P. (1994) Tropomyosin inhibits the glutaraldehyde-induced cross-link between the central 48-kDa fragment of myosin head and segment 48–67 in actin subdomain 2. *Biochemistry* **33**, 2594–2603.
66. Andreev, O.A. & Borejdo, J. (1995) Binding of heavy-chain and essential light-chain 1 of S1 to actin depends on the degree of saturation of F-actin filaments with S1. *Biochemistry* **34**, 14829–14833.
67. Andreev, O.A., Andreeva, A.L. & Borejdo, J. (1997) Cardiac actomyosin rigor complexes. *Biophys. J.* **72**, A52.